Chinese Journal of Structural Chemistry 43 (2024) 100235

Contents lists available at ScienceDirect

Chinese Journal of Structural Chemistry

journal homepage: www.journals.elsevier.com/chinese-journal-of-structural-chemistry

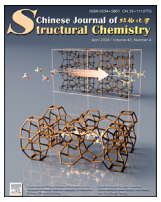

Short Communication

DNL-16: A new zeolitic layered silicate unraveled by three-dimensional electron diffraction

Chao Ma [a,b,c], Peng Guo [b,c,*], Zhongmin Liu [a,b,c]

[a] School of Chemistry, Dalian University of Technology, Dalian, Liaoning, 116024, China
[b] National Engineering Research Center of Lower-Carbon Catalysis Technology, Dalian Institute of Chemical Physics, Chinese Academy of Sciences, Dalian, Liaoning, 116023, China
[c] University of Chinese Academy of Sciences, Beijing, 100049, China

Two-dimensional (2D) zeolitic layered silicates (ZLSs) are drawing increasing attention since they have large external surface areas, easy convenience for further pillaring or exfoliating for desirable properties, and even promising candidates for constructing novel three-dimensional (3D) zeolites [1,2]. From the structural point of view, basic building units SiO_4 in ZLSs are interconnected through sharing the bridging oxygen atoms. Concurrently, the propagation of this tetrahedral network into a third spatial dimension is inherently restricted. In this case, the organic structure-directing agents (OSDAs) are occluded between ZLSs. Nowadays, a series of ZLSs have been successfully synthesized and extensively investigated [1,3–10]. For example, Kumar Varoon Agrawal's group reports a ZLS RUB-15 which can be easily exfoliated and calcined to construct 2D separation membranes for sieving performance with the H_2/CO_2 ideal selectivity [3]. ZLSs can also serve as precursors for synthesizing novel zeolites. The transformation of ZLSs into 3D zeolites is facilitated through the interlayer condensation of silanol groups, such as **CDO**, **NSI**, **RRO** and **RWR**-type zeolite frameworks [4,6–8]. Moreover, Corma's group proposes an innovative approach for creating zeolite-encapsulated sub-nanoplatinum species catalysts. This method utilizes ZLS MWW(P) as the initial material and then involves encapsulating the platinum species within ZLSs. This encapsulation occurs during the interlayer swelling and condensation process, ultimately leading to the formation of a highly stable 3D structured Pt@MCM-22 catalyst [5]. Consequently, the synthesis and structure of novel layered zeolites have been extensively studied.

From a synthetic perspective, these fascinating ZLSs can be synthesized using both monoquaternary ammonium compounds and diquaternary ammonium compounds [9,10]. The structural flexibilities and diversities of the latter enable us to synthesize not only 2D ZLSs but also intriguing 3D zeolites with diverse topologies. For example, the flexible pyrrolidine-based diquaternary ammonium has been considered as an efficient one for synthesizing novel zeolites as depicted in Fig. S1 (details in the Supporting Information).

Understanding the crystallographic structure is crucial for establishing the structure-property relationship in the field of ZLSs. Due to the tendency of ZLSs to crystallize at the nanometer scale, which is too small for conventional single-crystal X-ray diffraction techniques, powder X-ray diffraction (PXRD) is commonly employed for structure determination. However, challenges such as peak overlapping, undesirable impurities, and severe preferred orientation can complicate the process of structure determination. Currently, continuous rotation electron diffraction (cRED), a method within the scope of 3D electron diffraction (ED) techniques, is capable of solving the crystallographic structure from a single nanocrystal [11]. This technique allows for the determination of unit cell parameters, space group, and atomic coordinates from 3D cRED data, and thus has been successfully applied to elucidate the fine structures of novel zeolites [12–14].

Herein, we synthesized a new ZLS, named DNL-16, using hydroxide-type 1,4-bis(*N*-methylpyrrolidinium)butane (denoted as 1,4-MPBOH) as OSDA by adjusting the synthetic conditions such as the concentration of OSDA and the amount of water. The crystallographic structure of DNL-16 is unraveled by cRED. By using a combination of simulated annealing and Rietveld refinement against high-resolution PXRD data, we further determined 1,4-MPBOH locations between silicate layers.

DNL-16 was hydrothermally synthesized with the gel molar composition of $1.0SiO_2$:$13.0H_2O$:0.3 OSDA by using 1,4-MPBOH as OSDA. The PXRD results indicate that DNL-16 exhibits a high degree of crystalline purity (Fig. S2). Furthermore, SEM imaging demonstrated that DNL-16 has a plate-like morphology, as illustrated in Fig. S3. ^{13}C MAS NMR spectrum shows OSDAs maintain intact in the as-made sample (Fig. S4). The ^{29}Si MAS NMR analysis reveals that the peaks at −99.10 and −101.90 ppm are associated with Q^3 species, while those at −105.20,

* Corresponding author. National Engineering Research Center of Lower-Carbon Catalysis Technology, Dalian Institute of Chemical Physics, Chinese Academy of Sciences, Dalian, Liaoning, 116023, China.
E-mail address: pguo@dicp.ac.cn (P. Guo).

https://doi.org/10.1016/j.cjsc.2024.100235
Received 1 December 2023; Received in revised form 7 January 2024; Accepted 17 January 2024
Available online 19 January 2024

−109.10, and −115.20 ppm correspond to Q^4 species. In DNL-16, the proportion of Q^3 species is determined to be 41.92%, as shown in Fig. S5.

In order to solve the crystallographic structure of DNL-16, we collected ED data using the cRED technique and reconstructed 3D ED in reciprocal space (Fig. 1(a)). The 2D slices 0*kl*, *h*0*l*, and *hk*0 slices cut from 3D ED data are shown in Fig. 1(b–d). The triclinic unit cell is determined from the 3D ED data as: $a = 7.47$, $b = 9.10$, $c = 10.66$ Å, $\alpha = 86.6°$, $\beta = 74.8°$, $\gamma = 68.3°$, and the space group is deduced to be *P*-1. At a resolution of 0.85 Å, the completeness of this dataset can be 65.7%. The initial structural model of DNL-16 can be obtained by using SHELXT software, and the initial positions of 10 Si and 22 O atoms within the asymmetric unit can be obtained directly. In order to finalize DNL-16 structure, Rietveld refinement against high-quality PXRD data is employed (details in Fig. S7, Tables S1 and 2). Based on the combined analysis of TGA (Fig. S6) and ^{29}Si MAS NMR data, along with the structural information obtained, the unit cell composition of the DNL-16 sample is deduced to be $|(C_{14}H_{30}N_2)_{0.66}(H_2O)_{0.44}|[Si_{10}O_{19.32}(OH)_{2.68}]$.

In this work, the layer in DNL-16 is designated L0 for simplifying the following illustration (Fig. 2(a)). DNL-16 consists of *bre* composite building units (CBUs) (Fig. 2(b)) highlighted in Fig. 2(a), which was firstly identified in the natural zeolite brewsterite (**BRE**). In the **BRE** zeolite framework (Fig. S8(a)), the *bre* CBUs are connected to form a chain, labeled as C1. Adjacent C1 chains are then interconnected by alternating 4- and 6-rings, creating a building layer referred to as L1, as depicted in Fig. S8(b). These layers are subsequently connected to their neighboring layers, culminating in the formation of a 2D channel system characterized by 8 × 8-ring channels.

Through scrutinizing the zeolite structures deposited in the IZA database [15], there are another five frameworks including **HEU**, **RRO**, **STI**, **PWO**, and **PWW** constructed by *bre* CBU solely. The different connections of *bre* CBUs lead to distinct 3D zeolite structures (Fig. S8(c–j)).

Both **HEU** and **RRO** zeolite frameworks have identical building layer but different pore openings (Fig. S8(c and d)). The *bre* CBUs are connected by 4-rings to form the C2 chain. The C2 chain and its symmetry-related counterpart C2′ are joined by 5-rings to construct the L2 layer (illustrated in Fig. S8(e)). The L2 layer is further assembled by a mirror plane and an inversion center to form the **HEU** and **RRO** zeolite frameworks, respectively.

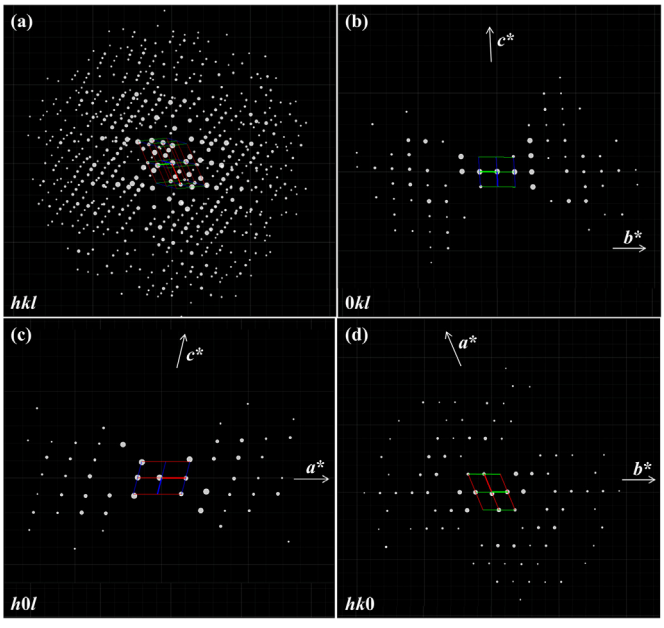

Fig. 1. (a) Reconstructed 3D reciprocal lattice of DNL-16 from the cRED data. (b–d) Three 2D slices 0*kl*, *h*0*l* and *hk*0 extracted from the reconstructed reciprocal lattice.

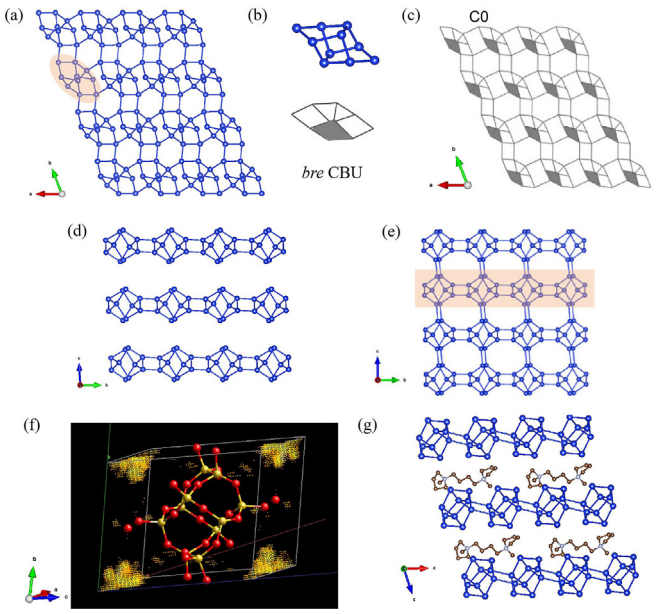

Fig. 2. (a) The structural model of DNL-16 along [001] and the highlighted *bre* CBU. (b) The *bre* CBUs in different styles. The bottom one is for the convenience to distinguish the orientations of *bre* CBUs. (c) The L0 layer identified in DNL-16. The adjacent *bre* CBUs are non-joint here. (d) The structural model of DNL-16 along [100]. (e) The hypothetical 3D structure constituted by the connection of L0 layers. (f) The difference electron density map between L0 layers through Rietveld refinement, indicating initial locations of OSDAs. (g) Final locations of OSDAs in the interlayers of DNL-16.

The **STI** framework features a 2D 10 × 8-ring channel system and is built from a distinct *bre* building layer, as depicted in Fig. S8(f). The *bre* CBU and its mirror image are connected to form the C3 chain. Then C3 chain and its symmetry-related one are further linked by 6-rings, resulting in the formation of L3 layer (Fig. S8(g)).

The **PWW** and **PWO** frameworks have identical *bre* building layer (Fig. S8(h and i)). The *bre* CBUs link together by bonding vertices, forming the C4 chain. The C4 chain and its symmetry-related one through a glide plane are further connected by alternating 4- and 5-rings, generating L4 layer (Fig. S8(j)). Unlike in L1, L2, and L3 layers, the adjacent *bre* CBUs are non-joint in the L4 layers, which are further assembled into **PWW** and **PWO** frameworks by a mirror plane and an inversion center, respectively.

Based on the aforementioned structural features of **BRE**, **HEU**, **RRO**, **STI**, **PWO**, and **PWW**, the L0 layer of DNL-16 turns out to be a unique and new one, as shown in Fig. 2(a). The *bre* CBUs in L0 connect with each other by 4-ring, constructing the chain C0. Then adjacent C0 chains are further connected by 6-ring, leading to the L0 layer (Fig. 2(b–d)). Besides, the adjacent *bre* CBUs in L0 layer are non-joint as well. This novel layer presents the opportunity to create a new 3D structure upon calcination of DNL-16, as illustrated in Fig. 2(e). The structure features a 2D 8 × 8-ring channel system between adjacent layers. Optimal calcination conditions are currently under investigation, as the most challenging issue stems from the condensation of Si–OH groups within the layer, impeding further interlayer connection. Rietveld refinement combined with the simulated annealing algorithms has been utilized to locate the atomic coordinates of OSDA. It shows that positions of 1,4-MPBOH are determined to be between adjacent L0 layer (Fig. 2(f and g)).

In conclusion, we successfully synthesize a novel ZLS, DNL-16, using 1,4-MPBOH as the OSDA. The unique layered structure of DNL-16, characterized by *bre* CBUs, is intricately unraveled using 3D ED. Further, the precise location of 1,4-MPBOH, situated between adjacent L0 layers of DNL-16, is determined through high-quality PXRD

complemented by Rietveld refinement. These findings not only reveal the complex structure of DNL-16 but also lay a foundational groundwork for future investigations into its potential applications.

Declaration of competing interest

The authors declare no competing interests.

Acknowledgements

This work is supported by the National Natural Science Foundation of China (Nos. 22288101, 21972136, 21991090, 21991091, and 22372156).

Appendix A. Supplementary data

Supplementary data to this article can be found online at https://doi.org/10.1016/j.cjsc.2024.100235.

References

[1] E. Doustkhah, Y. Ide, Microporous layered silicates: old but new microporous materials, New J. Chem. 44 (2020) 9957–9968.
[2] T. Selvam, A. Inayat, W. Schwieger, Reactivity and applications of layered silicates and layered double hydroxides, Dalton Trans. 43 (2014) 10365–10387.
[3] M. Dakhchoune, L.F. Villalobos, R. Semino, L. Liu, M. Rezaei, P. Schouwink, C.E. Avalos, P. Baade, V. Wood, Y. Han, M. Ceriotti, K.V. Agrawal, Gas-sieving zeolitic membranes fabricated by condensation of precursor nanosheets, Nat. Mater. 20 (2021) 362–369.
[4] T. Ikeda, Y. Akiyama, Y. Oumi, A. Kawai, F. Mizukami, The topotactic conversion of a novel layered silicate into a new framework zeolite, Angew. Chem. Int. Ed. 43 (2004) 4892–4896.
[5] L. Liu, U. Díaz, R. Arenal, G. Agostini, P. Concepción, A. Corma, Generation of subnanometric platinum with high stability during transformation of a 2D zeolite into 3D, Nat. Mater. 16 (2017) 132–138.
[6] S. Zanardi, A. Alberti, G. Cruciani, A. Corma, V. FornØs, M. Brunelli, Crystal structure determination of zeolite Nu-6(2) and its layered precursor Nu-6(1), Angew. Chem. Int. Ed. 43 (2004) 4933–4937.
[7] Y.X. Wang, H. Gies, B. Marler, U. Muller, Synthesis and crystal structure of zeolite RUB-41 obtained as calcination product of a layered precursor: a systematic approach to a new synthesis route, Chem. Mater. 17 (2005) 43–49.
[8] B. Marler, N. Ströter, H. Gies, The structure of the new pure silica zeolite RUB-24, $Si_{32}O_{64}$, obtained by topotactic condensation of the intercalated layer silicate RUB-18, Microporous Mesoporous Mater. 83 (2005) 201–211.
[9] J.E. Schmidt, D. Xie, M.E. Davis, Synthesis of the RTH-type layer: the first small-pore, two dimensional layered zeolite precursor, Chem. Sci. 6 (2015) 5955–5963.
[10] S. Li, L. Han, Z. Zhao, H. Xu, J. Jiang, P. Wu, Zeolites featuring 14 × 12-ring channels with unique adsorption properties, Inorg. Chem. Front. 8 (2021) 5277–5285.
[11] Y. Wang, S. Takki, O. Cheung, H. Xu, W. Wan, L. Öhrström, A.K. Inge, Elucidation of the elusive structure and formula of the active pharmaceutical ingredient bismuth subgallate by continuous rotation electron diffraction, Chem. Commun. 53 (2017) 7018–7021.
[12] J. Wang, C. Ma, J. Liu, Y. Liu, X. Xu, M. Xie, H. Wang, L. Wang, P. Guo, Z. Liu, Pure silica with ordered silanols for propylene/propane adsorptive separation unraveled by three-dimensional electron diffraction, J. Am. Chem. Soc. 145 (2023) 6853–6860.
[13] J. Li, Z. Gao, Q. Lin, C. Liu, F. Gao, C. Lin, S. Zhang, H. Deng, A. Mayoral, W. Fan, S. Luo, X. Chen, H. He, M.A. Camblor, F. Chen, J. Yu, A 3D extra-large-pore zeolite enabled by 1D-to-3D topotactic condensation of a chain silicate, Science 379 (2023) 283–287.
[14] Z. Huang, T. Willhammar, X. Zou, Three-dimensional electron diffraction for porous crystalline materials: structural determination and beyond, Chem. Sci. 12 (2021) 1206–1219.
[15] https://asia.iza-structure.org/IZA-SC/ftc_table.php.